Environmental Sciences Europe

RESEARCH Open Access

Radiological survey on radon entry path in an underground mine and implementation of an optimized mitigation system

Amin Shahrokhi* and Tibor Kovacs

Abstract

Background: The European Union council has introduced the basic safety standards (EU-BSS) for protection against the dangers arising from exposure to ionizing radiation by laying down a new radon reference level at workplaces. In this regard, all European state members must establish a national reference level based on all pre-defined requirements. After implanting the directive 2013/59/Euratom by European state members, new challenges have been revealed to mitigate radon appropriately in underground workplaces due to the exciting limitations (e.g., ventilation system, dust dispersion, air injection, etc.). Therefore, a conceptual design of an environmental radiological survey was defined and implemented by examining the hypothesis to find practical solutions following EU-BSS. The main objectives of this study were to identify the potential radon entry paths, utilize an optimized ventilation system, and carry on long-term radon monitoring in an operational underground manganese mine.

Results: The mullock rocks (the geological structure of the mine walls) contained a small amount of Ra-226 (2–4 Bq kg^{-1}). On the other hand, the mine ore (black shale, underlayer black shale, and carbonate ore) has shown the highest concentration of Ra-226 (12–16 Bq kg^{-1}) and the highest radon exhalation (1.2–1.6 mBq s^{-1} m^{-2}). The surface radon exhalation from the mine walls was in the range of 0.7 ± 0.1 and 1.5 ± 0.2 mBq m^{-2} s^{-1}. It was found that shortly after mining activity was undertaken, radon concentration increased dramatically with an average of about 5900 ± 420 Bq m^{-3} near the freshly broken walls. The optimized mobile mitigation system reduced radon concentration to 250 ± 41 Bq m^{-3} on average.

Conclusion: Apart from the fact that aged walls were involved in the radon accumulation, considering the mine ventilation performance and the total active surface area, the exhaled radon from the aged walls could not be the primary potential source of high radon concentration when mining activity was undertaken. According to the obtained results, the ores, recently fragmented during the course of mining operations, were the primary path. Therefore, after successfully identifying the radon entry path, radon concentration could be reduced to meet the EU-BSS requirement by implementing the developed mitigation system.

Keywords: EU-BSS, CR-39, Gamma spectrometry, Exhalation, Manganese mine, Mitigation

Background

Radon is a radioactive and inert gas that can migrate from soils and rocks and accumulate in enclosed areas (i.e., underground mines and caves). Radon itself is an alpha emitter, but the radiological concern is due to its short-lived alpha emitter decay products. It was found that in the miners, about 40% of all lung cancer deaths might be due to exposure to radon and radon decay products, 70% of lung cancer deaths in never-smokers, and 39% of lung cancer deaths in smokers [1, 2]. This can be due to the condition of mines, e.g., if a miner had continuous exposure to 1 working level month for a year (WLM_{Annual}) in

*Correspondence: ashahrokhi@almos.uni-pannon.hu
Department of Radiochemistry and Radioecology, University of Pannonia, Veszprém, Hungary

a mine, this is comparable to exposure over 1 year in a dwelling with a radon concentration of 230 Bq m^{-3} [3, 4].

Radon presence in the mine atmosphere is almost prevalent and relatively unavoidable. The source can come from trace concentrations of uranium on the ground (ore, host rock, organic material, and soils) or through the exhalation from radon/radium contained in the groundwater. Therefore, the radon concentration in an underground mine environment mainly depends on radon emissions from the ore body, broken ore, host rock, and underground water. On the other hand, recent studies show that the remaining radon in an enclosed area for a more extended period generates a higher concentration of radioactive decay products. Therefore, a rapid air change can quickly reduce the radon gas concentration inside the mine and result in a lower quantity of radon decay products building up, in addition to lowering aerosol concentration. Therefore, radon progeny concentration within underground mines depends on the fresh air exchange rate and ventilation. Monitoring and measuring radon concentration in dwellings,public areas and underground workplaces have been the expert's concern foryears [5–12].

Úrkút manganese mine is located near the village of Úrkút in the Balaton upland region of Hungary. Manganese ore extraction from the Bakony Mountains was started in the Early 20th Century [13, 14]. The Bakony Mountains are an important region for structurally controlled black shale-hosted Manganese mineralization of the Jurassic age in Hungary. The Úrkút manganese ore deposit (Úrkút Manganese Formation—ÚMnF) is surrounded by mountains of the Alps and Carpathians in Pannonian Basin and belong to tectonically of the North Pannonian unit (Fig. 1). Mining in Úrkút mountains to extract manganese ore was going on from 1917 until 2017.

In addition to the natural air exchange (a process that resulted from the difference in the pressure and temperature between the underground atmosphere (186 m) and surface by shafts), the inside air was purified using a central ventilation system during working hours. A vent blows fresh air through a canvas or pipes (average airflow of 60,000 $m^3 \cdot h^{-1}$) into a 6-km-long galleries system (draught between the two shafts by a central fan). For those places where using central ventilation was not possible (e.g., blind galleries, faces, galleries under construction, etc.), auxiliary ventilation was used to exchange the air.

The Úrkút manganese mine was under attention for the first time in middle 2002. The first study was conducted to determine if there was a health risk for workers exposed to radionuclides in the mine during working time based on the standards and regulations. It was indicated that the only direct potential hazard health could be the accumulated radon in the air. Therefore, increasing the ventilation rate was suggested as a solution, but that was not possible due to the Hungarian regulation. On the other hand, increasing the airflow would increase the resuspension and circulation of dust inside the mine and causing added health problems. The average radon concentration was kept below 1000 Bq m^{-3} by decreasing working hours and increasing the ventilation rate to the maximum permitted level. That was a practical solution until 2013, when Europe established a new regulation to keep radon concentration in dwellings and work areas below 300 Bq m^{-3}.

Since it was not possible to increase the ventilation flow rate (due to the workplace regulation and conditions), and natural air exchange and central ventilation were not effective enough, an effective mitigation system was needed in active ore production sites. These faces were vital as they were the most intensive workplaces involving many workers.

According to the European Union Basic Safety Standards timeline—EU BSS—[15], all EU members should apply the requirements by starting 2018. Reducing radon concentration to below the recommended level can be a new challenge for the work areas, such as underground mines and caves. Therefore, in this study, to meet the EU-BSS, it was tried to find out the problems and solutions for underground workplaces. The first step to control radon concentration in an environment is to recognize the source. By following, optimization of ventilation can be another way of reducing the radon concentration.

The objectives of this work were (i) to find the primary radon entry source in the mine and (ii) to use an optimized mobile ventilation system inside the mine, to meet the EU-BSS requirements. The results related to the effect of dissolved radon in water and the radon diffusion coefficient from water to the mine air will be published in another paper.

Materials and methods

A conceptual survey was designed to collect data from radon exhalation before and after implementing a new mitigation system, as depicted in Fig. 2.

Radon monitoring

Radon measurement was divided into two different methods of passive and active monitoring. The methodology of these measurements could be found in the previously published papers [16–19].

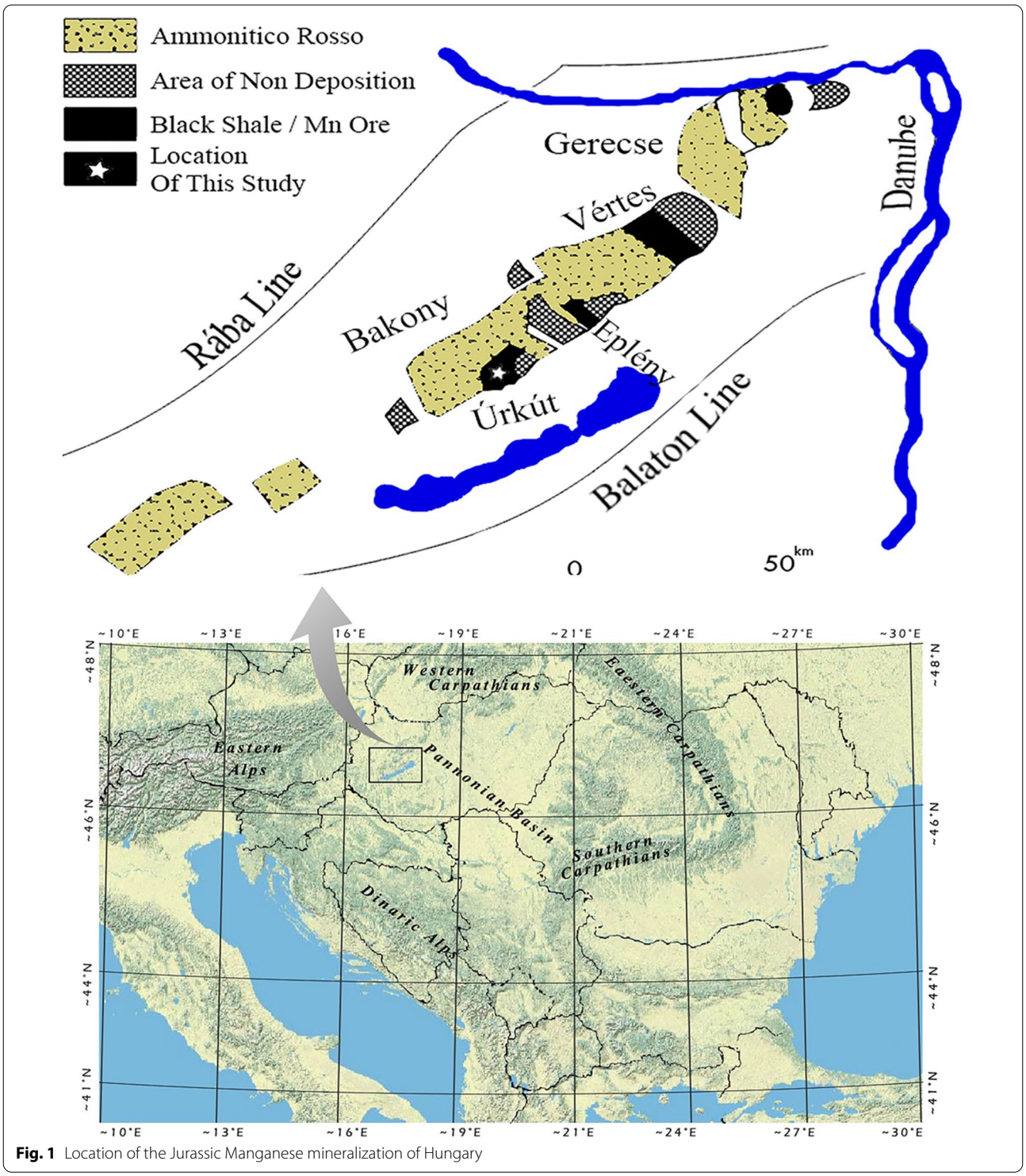

Fig. 1 Location of the Jurassic Manganese mineralization of Hungary

In situ and ex situ measurements

Continuing our previous experiment [17], six different rock types were collected for gamma spectrometry and aerial radon exhalation measurements (ex situ), in addition to the in situ radon exhalation measurements. The experiment was divided into two phases. In the first step, a series of extensive measurements was carried out to directly estimate the radon exhalation from mine walls with the extent of 50 to 200 m from each measured location. Secondly, a group of 32 samples (including six

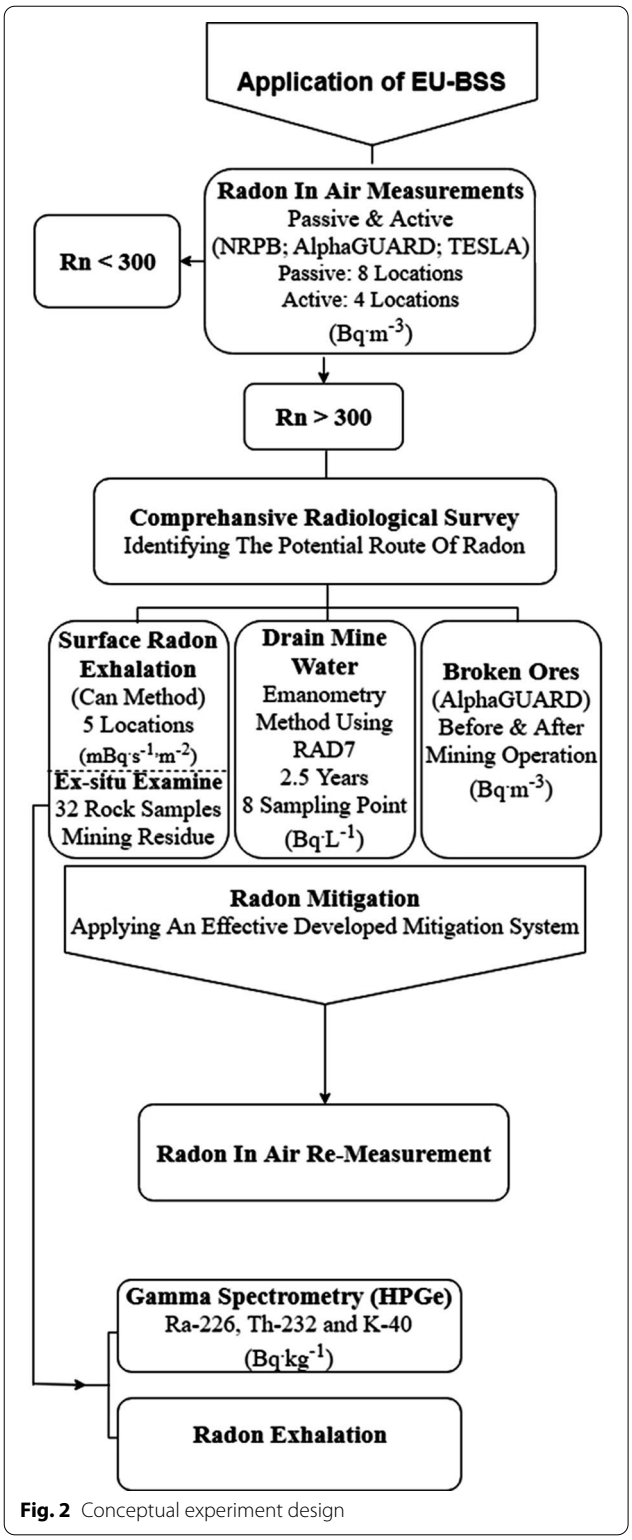

Fig. 2 Conceptual experiment design

most abundant rocks) from the mine's walls was collected and transferred to the laboratory to measure the specific radon exhalation. Besides, gamma spectrometry was used to identify and quantify the radionuclides in the rock samples. The quantity of Ra-226 in the samples can help get an overview of radon exhalation from the surface materials. Although measuring K-40 was not in the scope of this study, it is a standard process to measure it in radiological surveys. Additionally, due to the different migration behavior of K-40 and Ra-226, it might help to make a perspective view when there is a high variation of Ra-226 between the rocks of the same family type.

Gamma spectrometry

A high-resolution gamma-ray spectrometer, equipped with an ORTEC GMX 40–76 HPGe semiconductor radiation detector with the relative efficiency of 40%, was used to evaluate all gamma-emitting components, both by quality and quantity through the detection of the amplitude and energy level of the emitted gamma photons from isotopes, and hence determining the specific activity concentration of the radionuclides (Th-232 (Ra-228), Ra-226 and K-40) in the rock samples. The detector was covered with a 20-cm-thick lead shield and a layer of nickel all around to decrease the natural background rate. Data were analyzed by Aptec MCA Multichannel Analyzer software. More details regarding the gamma-ray measurement used in this study can be found [20–22]. The detector is regularly calibrated following the IAEA protocols. Related information regarding the calibration process is presented in a previous publication [23]. For quality assurance (QA) purposes in the analytical protocol, a certified soil standard, provided by the International Atomic Energy Agency with a known activity concentration of various radionuclides, was used.

A portion of each sample (1 kg) was stored at room temperature for several days and dried in a ventilated oven at 125 °C for 24 h to reach a constant weight. Samples were pulverized and sieved to less than 0.3 mm to the same size as the reference material (IEA-375, Soil standard). 500 g of each homogenized sample were separately filled into an air-tight Marinelli beaker. The beakers were sealed for 29 days to reach secular equilibrium between Ra-226 and Rn-222 and its short-lived decay products before being counted by gamma spectrometry.

The activity concentration of each radionuclide was determined using the specific gamma peaks. For K-40, the peak energy 1460.8 keV (Pγ: 10.6%). For Ra-226, the peak energies of its decay products Pb-214 and Bi-214, 351.9 keV (Pγ: 35.3%) and 609.3 keV (Pγ: 45.2%), respectively. Th-232 was calculated by the weighted mean value of Ra-228 and Th-228 concentration using its decay products in an equilibrium condition when the activity of Ac-228 is equal to the activity of Pb-212. In case of no equilibrium condition, just Th-228 would be considered. For Ra-228, the two peak energies of its decay

product Ac-228, 911.2 (Pγ: 26%) and 969 keV (Pγ: 16%). For Th-228, the peak energies of its decay products Tl-208 and Pb-212. The peak energies of 583.2 and 2614.5 keV (Pγ: 30.5% and 35.8%) for Tl-208. For Pb-212, the peak energy of 238.6 keV (Pγ: 43.6%).

Radon exhalation

Surface radon exhalation measurements were carried out using the CR-39 based can method (radon accumulation chamber method) with dimensions of 6 cm (height) and 11 cm (diameter) covering a total surface of 95 cm^2. The cans were sealed on the surface of the mine wall in 5 different locations for 3 weeks. This method is based on trapping the exhaled radon from the surface and growth inside the accumulation chamber (Fig. 3).

Detectors were placed in the exact location where most miners were working there. The cap was sealed on the surface of the mine wall. At the time of placing the detectors, three detectors were kept in the laboratory to evaluate the background.

As the surface radon exhalation focuses on this section, the diffusion process can be assumed to take place in one dimension along with the thickness of the wall towards the surface. As the radon atoms reach the surface of the wall, exhalate and enter the air. It is known as surface radon exhalation and can be calculated using Eq. 1, expressing the correlation between accumulated radon and the radon exhalation:

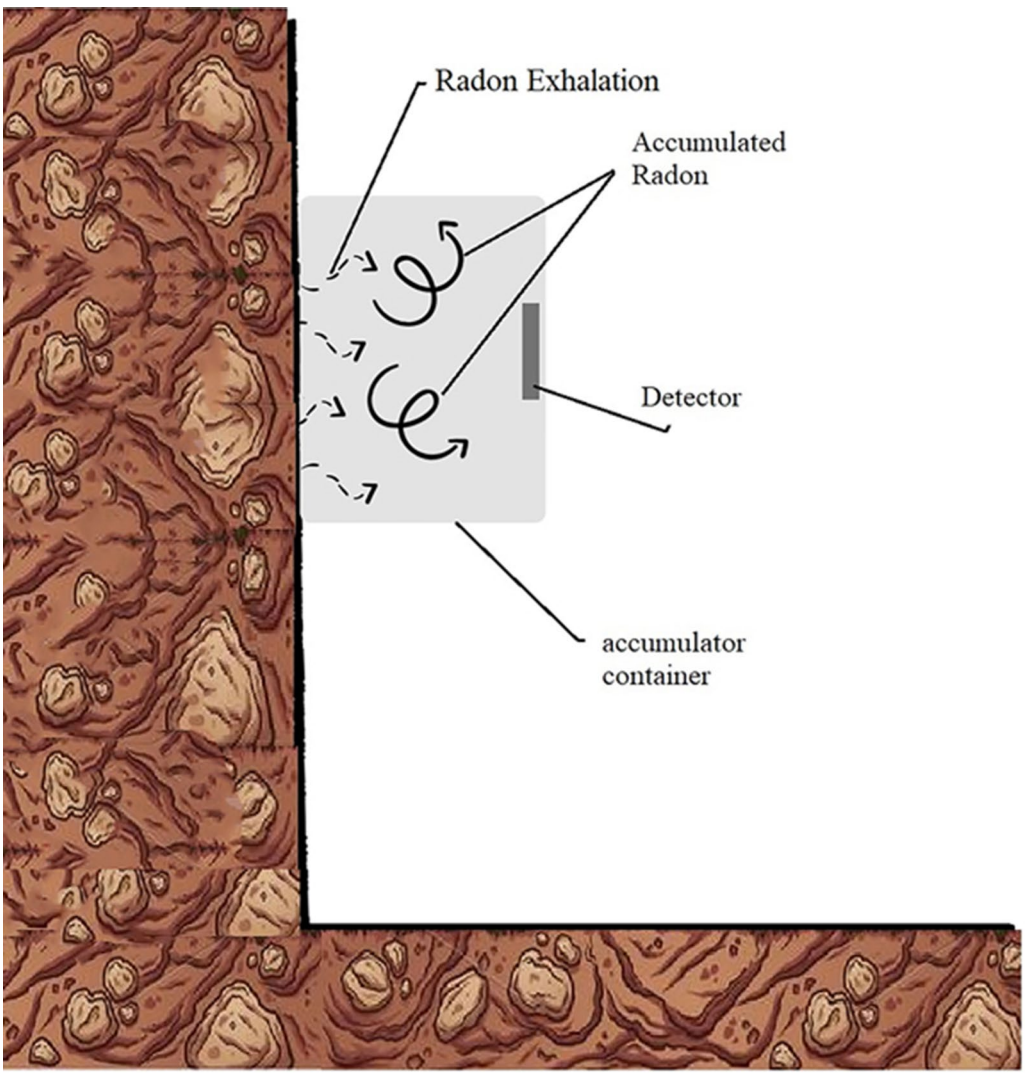

Fig. 3 Radon exhalation measurement based on the can method

$$C_{\mathrm{Rn}} = \left(\frac{E_{\mathrm{Rn}} S}{V(\lambda + L_{\mathrm{Rn}})}\right)\left(1 - e^{-\lambda t}\right), \quad (1)$$

where C_{Rn} is the accumulated radon concentration for a period of t (Bq m^{-3}), S is the canister base area (m^2), E_{Rn} J is the radon exhalation rate (Bq m^{-2} s^{-1}), L_{Rn} (s^{-1}) is the chamber leakage coefficient (which is~ 0 in this study), V is the total canister volume (m^3), t is the time since sealing (s), λ is the decay constant of radon (s^{-1}).

Simplifying Eq. 1, assuming knowing the accumulated radon concentration in terms of the accumulation period, gives Eq. 2 to estimate radon exhalation for a specific area:

$$E_{Rn} = \frac{C_{\mathrm{Rn}} \lambda \left(\frac{V}{S}\right)}{1 - e^{-\lambda t}}. \quad (2)$$

For ex situ radon exhalation measurements, each sample was separately stored and sealed in a leak-proof box, Fig. 4, (leakage rate = 0), waiting for a period of 24 to 27 days to accumulate exhaled radon. An AlphaGUARD (PQ2000, Saphymo Gmbh, Germany), a portable radon monitor, was connected to the chamber as a loop system. The pump was running for about 15 min to reach equilibrium in the system (AlphaGUARD, pump, pipes, and container). Then the pump was turned off and waited for 2 to 5 min to clear the influence of thoron (Rn-220), and then the measured radon concentration was recorded.

The aerial radon exhalation (ERn) from samples was determined using Eq. 3:

$$E_{\mathrm{Rn}} = \frac{C(V_1 + V_2 + V_3 + V_4)\lambda}{A\left[T + \frac{1}{\lambda}(e^{-\lambda t} - 1)\right]}, \quad (3)$$

where V_1, V_2, V_3, V_4 are the volume of the container, AlphaGUARD, pump and pipes, respectively, C is the radon concentration in (Bq m^{-3}), A is the available radon exhalation area (m^2), and T is the irradiation time (s).

Fig. 4 Ex situ radon exhalation measurement system

Mobile mitigation system

As radon exposure is an issue of major concern to public health, the EU_BSS introduced a recommendation level of 300 Bq m^{-3}. Thus, any radon concentration above this level needs mitigation. Since it was not possible to increase the ventilation flow rate (due to the Hungarian workplace regulation and conditions), and the natural air exchange rate was not effective enough, an optimized mobile mitigation system was used at the active ore production sites. Therefore, a functionally developed air injection system based on the existing ventilation system was adopted.

The forced ventilation system was used in the galleries every 200 m and the galleries longer than 15 m. The natural diffusion was responsible for radon mitigation for the new galleries where mining activity already occurred or was occurring. In this system, a flexible plastic tube with a length of several centimeters (when it was compressed) up to 200 m (when it was extended) with a diameter of about 460 mm was used to plug into the last connector of the forced ventilation. Therefore, extending the tube to the new galleries as near as possible to the freshly extracted walls and by injecting fresh air (with a flow rate in the range of 50 up to 100 m^3 min^{-1}) was expected to result in an immediate radon reduction.

Results and discussion

The mine was operated in one working shift, 8 h per day and 5 days a week (working days). The average temperature and relative humidity were measured at about 13 ± 3 °C and 84 ± 6% (the values were almost constant during the year). To comply with the regulations and recommendations of the EU-BSS, firstly, it was necessary to find the primary entry source of radon in an area. Then, finding a solution to mitigate radon can be easier by removing the source or using other methods to reduce radon at the origin. Usually, mine walls, freshly broken ores, and backfill tailings are the primary sources of radon exhalation into the underground mine atmosphere. The radon concentration in the Úrkút mine was previously estimated [17], "The annual integrated averages radon concentration in whole mine area was 824 ± 42 Bq m^{-3}, 874 ± 45 Bq m^{-3} and 1050 ± 85 Bq m^{-3} for years 2014, 2015 and 2016, respectively".

Gamma spectrometry

Three main naturally occurring radionuclides (K-40, Th-232 and Ra-226) were considered for gamma

spectrometry. The specific peak detection efficiencies were determined for K-40, Ra-226, and Th-232 as 1.2%, 2.4%, and 1.4%, respectively. The minimum detectable activity of the same radionuclides, based on the observed data from background measurement, was calculated at 23, 0.5, and 0.7 Bq kg^{-1}, respectively. Table 1 shows the concentration of natural radionuclides in the rock samples (dry weight).

Activities of Ac-228 and Pb-212 were similar, so it can be assumed that Ra-228 and Th-228 were in secular equilibrium with the parent nuclide Th-232, which is not uncommon in these sorts of mineral samples. Activity concentrations of Th-232 and Th-228 were assumed to be equal.

After statistical analysis, it was observed that Dogger limestone had the lowest concentrations of Ra-226, Th-232 and K-40 among the other rock types with an average of 2 ± 1, 5 ± 1 and 72 ± 12 Bq kg^{-1}, respectively. The underlayer black shale showed the highest values with an average of 16 ± 4, 19 ± 5 and 432 ± 74 Bq kg^{-1}, for Ra-226, Th-232 and K-40, respectively.

Additionally, black shale and carbonate ore showed high values of Ra-226 compared to other samples. The concentration of Ra-226 was higher than the mean value in 47% of the samples. In comparison, Th-232 was above the average concentration in 44% of the samples. The highest activity concentration of Ra-226 was

Table 1 Concentrations of natural radionuclides in the mine rock samples (Bq kg^{-1})

					Min.–Max			Average		
Samples		**Ra-226**	**Th-232**	**K-40**	**Ra-226**	**Th-232**	**K-40**	**Ra-226**	**Th-232**	**K-40**
Carbonate (Mn ore)	C-1	15 ± 4	7 ± 2	245 ± 40	15–18	7–25	244–245	16	16	245
	C-2	18 ± 4	25 ± 5	244 ± 42						
Underlayer limestone (mullock)	F-1	4 ± 1	6 ± 2	45 ± 9	2–6	5–8	45–102	4	6	75
	F-2	4 ± 1	7 ± 2	62 ± 12						
	F-3	2 ± 1	8 ± 2	84 ± 13						
	F-4	6 ± 2	5 ± 1	102 ± 17						
	F-5	4 ± 1	5 ± 1	83 ± 14						
Dogger limestone (mullock)	D-1	2 ± 1	6 ± 2	88 ± 14	2–3	2–7	54–95	2	5	72
	D-2	2 ± 1	7 ± 2	95 ± 16						
	D-3	3 ± 1	2 ± 1	66 ± 11						
	D-4	2 ± 1	5 ± 1	54 ± 10						
	D-5	2 ± 1	3 ± 1	58 ± 10						
Black shale (Mn ore)	B-1	18 ± 5	21 ± 6	299 ± 50	9–18	15–21	266–456	12	19	375
	B-2	9 ± 2	16 ± 4	345 ± 60						
	B-3	12 ± 3	15 ± 4	266 ± 45						
	B-4	10 ± 3	16 ± 4	315 ± 54						
	B-5	13 ± 4	20 ± 6	456 ± 78						
	B-6	13 ± 4	18 ± 5	438 ± 74						
	B-7	11 ± 3	21 ± 5	451 ± 76						
	B-8	11 ± 3	19 ± 4	398 ± 69						
	B-9	13 ± 4	20 ± 5	415 ± 70						
	B-10	10 ± 3	20 ± 5	365 ± 62						
Underlayer black shale (Mn ore)	UB-1	11 ± 3	13 ± 3	255 ± 43	11–21	12–26	218–724	16	19	432
	UB-2	21 ± 6	22 ± 6	345 ± 58						
	UB-3	18 ± 4	26 ± 7	218 ± 38						
	UB-4	20 ± 6	22 ± 5	654 ± 110						
	UB-5	11 ± 3	12 ± 3	724 ± 123						
Puce greenish Marl (mullock)	R-1	4 ± 1	8 ± 2	66 ± 10	3–6	6–8	66–84	4	7	74
	R-2	3 ± 1	8 ± 2	74 ± 13						
	R-3	4 ± 1	8 ± 2	84 ± 15						
	R-4	5 ± 2	7 ± 2	78 ± 14						
	R-5	6 ± 2	6 ± 2	69 ± 13						

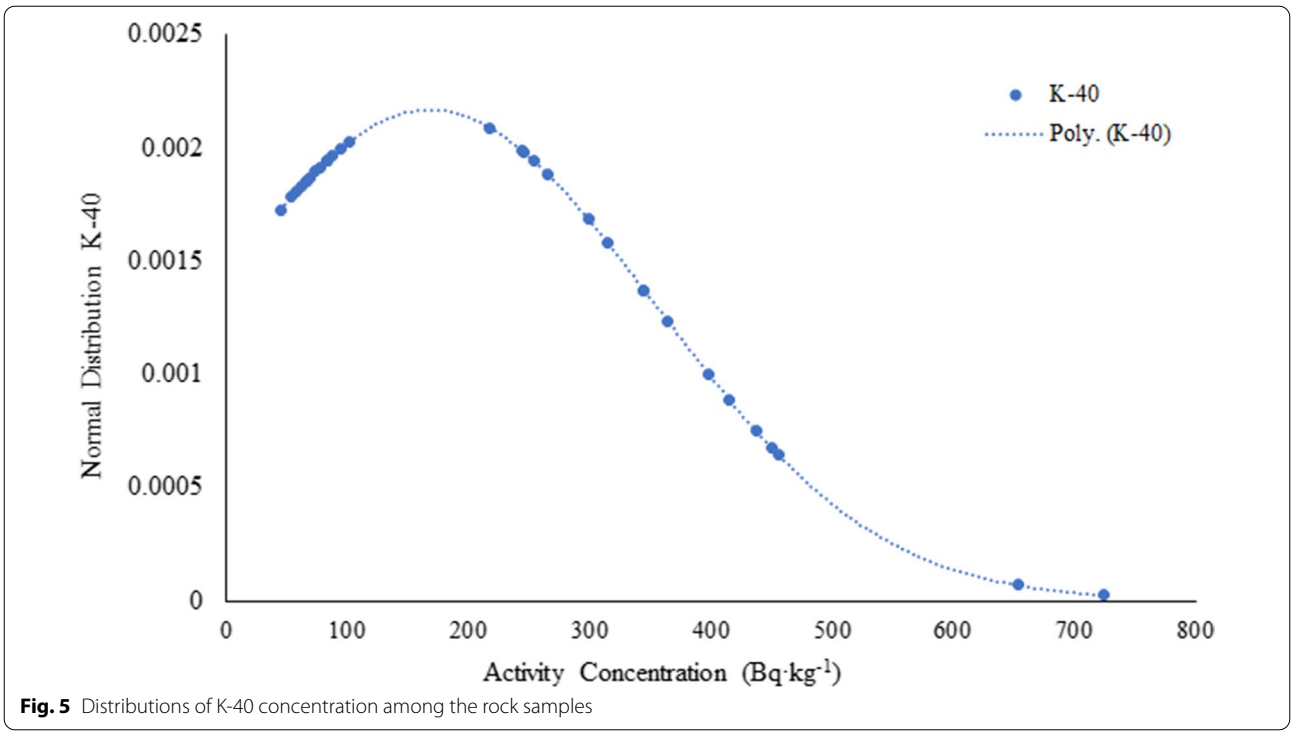

Fig. 5 Distributions of K-40 concentration among the rock samples

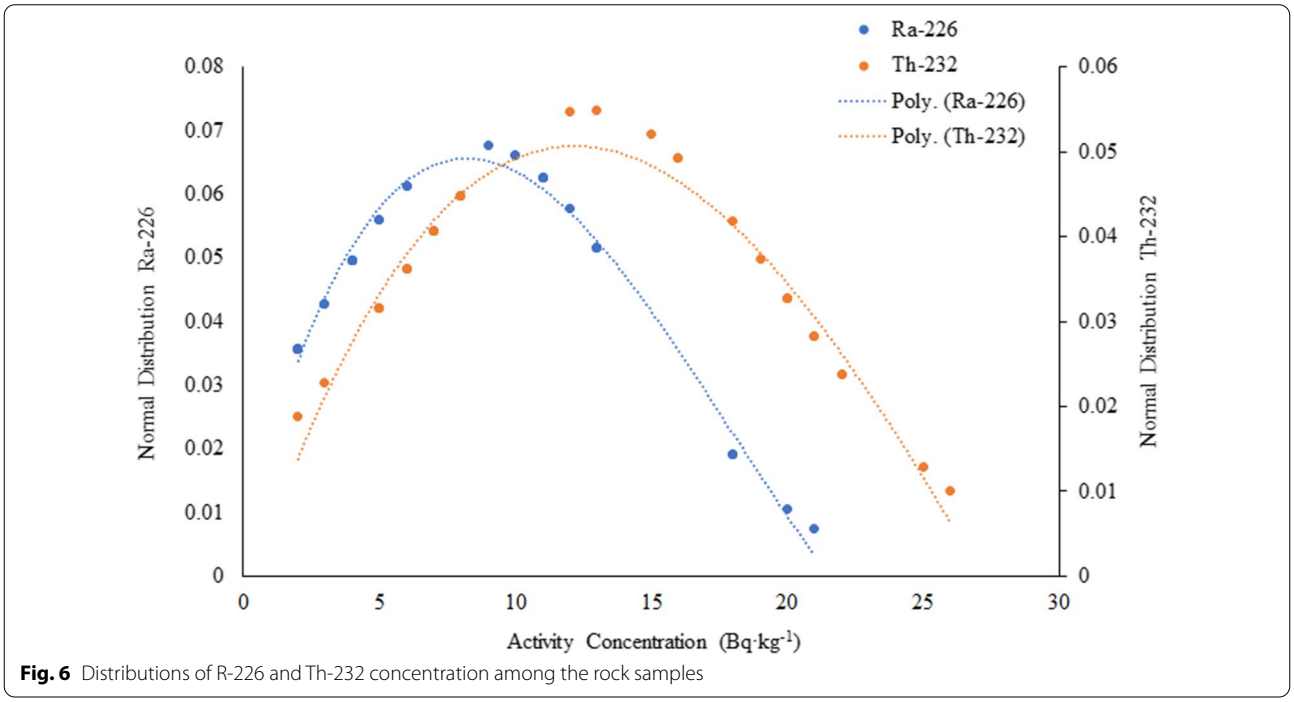

Fig. 6 Distributions of R-226 and Th-232 concentration among the rock samples

found in underlayer black shale samples. Figures 5 and 6 are shown the normal distribution and the standard deviation of the measured radionuclides' concentration among the samples.

Most of the K-40 distribution is in the range of ~ 50 and ~ 300 Bq kg^{-1}, while the values for Ra-226 and Th-232 are between ~ 3 and ~ 15 Bq kg^{-1} and ~ 10 and ~ 30 Bq kg^{-1}, respectively.

The highest normal distribution values for K-40, Ra-226, and Th-232 were calculated around 0.002, 0.07, and 0.05, respectively.

The correlations between the radionuclides among all the samples, as a single geological structure component of the mine wall, are shown as scatter plots of Th-232 vs. Ra-226, K-40 vs. Ra-226 and K-40 vs. Th-232 in Fig. 7.

A detailed analysis of the results indicates some degree of positive correlation between the activity concentrations of all measured radiological parameters. A comparison between concentrations of Ra-226 (found in this study) and U-238 concentration [24], for the same family of rocks and mine, is summarized in Table 2.

Radon exhalation measurements

One significant source of radon entry into the mine area is diffusion through the mineral-bearing host rock and subsequent exhalation through the mine walls. Radon, generated from Ra-226 presented in the mine wall rocks, diffuses to the surface area and then exhalate to the mine atmosphere. However, the exhalation can depend on ore grade, atmospheric condition, and other factors. Radon exhalation in the underground mine is due to (i) the old broken rocks (mine wall) and (ii) the freshly broken ore and wall from mining activities. The measurements are described below in two parts as in situ and ex situ measurements.

Aerial radon exhalation

Samples in different cylinder lengths were used to measure the radon exhalation from each rock type in terms of sample thickness. The aerial radon exhalation measurement is of prime importance in determining the contribution of every kind of rock in radon exhalation. The overall average values of radon exhalation from samples in terms of their thickness are shown in Fig. 8.

Carbonate ore, as was expected, showed the highest exhalation rate, as it contained the highest Ra-226 concentration among the other rock types. Puce greenish marlstone shows the lowest radon exhalation. It needs to be mentioned that radon exhalation directly depends on the moisture in the grain's pores and has an inverse relationship with grain size [25, 26].

The radon exhalation rate is going to reach a constant value by increasing the thickness of the samples. The high moisture content of the samples can be a reason for this behavior, as the water could be considered a deterrent to radon diffusion. Radon exhalation can reach a constant rate from 1 to several meters of sample thickness in dry samples, depending on the samples material. Várhegyi et al. [27] found that radon exhalation can reach a constant rate at a specific thickness of sand, depending on the moisture. In other words, moisture influences radon exhalation. The soil moisture content has a deterrent influence on the radon emanation coefficient by filling the pores and space within material's grains, resulting in a temporary blockage of emanated radon from grains to pores space (radon solubility in water may also aid in the release of radon trapped in pores) and/or radon diffusion from pores to surface [28, 29].

Surface radon exhalation

The quantitative estimation of the seasonal radon exhalation from the wall was made by measuring the build-up of radon concentration in accumulation chambers in 5 different mine locations. The geological characterization of the rocks presents in the mine galleries consists of different types of limestone and marl (Cherty limestone, Greenish grey calcareous marl, etc.), so it is difficult to isolate pure rocks due to the mixture above-mentioned. Table 3 summarizes the surface radon exhalation from the wall per location.

The surface radon exhalation was in the range of 0.7 ± 0.1 mBq $m^{-2} \cdot s^{-1}$ and 1.5 ± 0.2 mBq m^{-2} s^{-1}, with an average of 1.1 ± 0.1 mBq m^{-2} s^{-1}. Also, some variations between each measuring period for the exact location were observed, probably resulting from precipitation. As results show, high precipitation in rainy seasons might be the reason why the radon exhalation from the mine wall was lower than in dry seasons. And that can be due to high moisture content in the rock and soils, functioning as a deterrent factor [25]. In March, August, October, February, the average precipitation for this region was about 33, 62, 53, 32 mm, respectively. Likewise, the monthly average outdoor temperature was measured around 5, 22, 10 and 2 °C, respectively.

Regarding the results, in some locations, the radon exhalation could reach up to two times higher than the lowest exhalation value in other locations. It can be due to the rocks' mineralization feature on the mine wall. Therefore, to figure out the contribution of different rocks following a previous study, the authors carried out second measurements.

Interesting results were obtained from measurements in two mine walls of different ages. Continuous radon monitoring (real-time measurement) was conducted some days before starting new mining activity. An AlphaGUARD radon monitor device was connected to an accumulation chamber in the wall about 70 cm above the floor. Radon concentration was monitored in flow mode with hourly measurement cycles. This phase of measurement was named point "A" (aged wall). Another experiment was carried out after mine activity on the freshly broken wall in the exact location, called point "B" (Fresh broken wall or ore). Measurements were continued until released radon reduced up to its original value at point

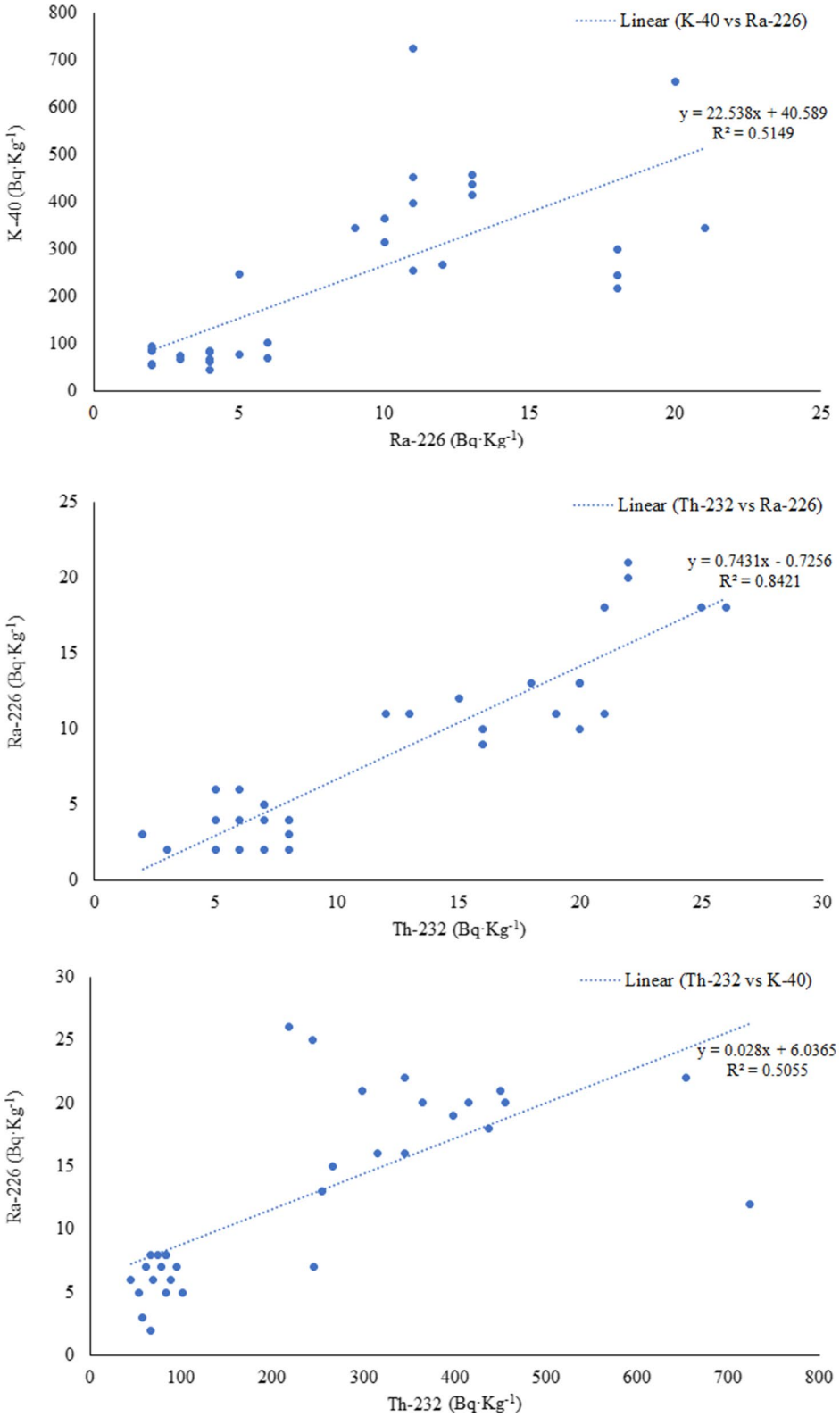

Fig. 7 Scatter plots of Th-232 vs. Ra-226; K-40 vs. Ra-226 and K-40 vs. Th-232

Table 2 Comparison of the Ra-226 and U-238 concentration among rock samples

Rock type	U-238 (Bq kg^{-1})	Ra-226 (Bq kg^{-1})
Carbonate ore	1–3 (1.6)	15 & 18 (16)
Black shale	5	9–18 (13)
limestone	1–2 (1.6)	2–6 (3)
Marlstone	1 & 4	3–6 (4)

"A". Figure 9 shows the measurement results as a function of time and radon concentration in each point of time marked on the graph.

As shown in Fig. 9, the radon concentration in the air directly depends on the broken ore (wall) age; (A) represents radon concentration near the old mine wall with an average of about 850 ± 125 Bq m^{-3}. Exactly after mining activity being restarted, the radon released from the exact location with the freshly broken wall (B) increased dramatically with an average of about 5900 ± 420 depending on the broken surface. This increase dropped down near 3300 ± 365 Bq m^{-3} by getting aged (depending on the broken surface area, it could last from 1 week to several weeks). Then radon concentration came back to its constant value (D). This could be due to releasing trapped or accumulated radon between pores and grains.

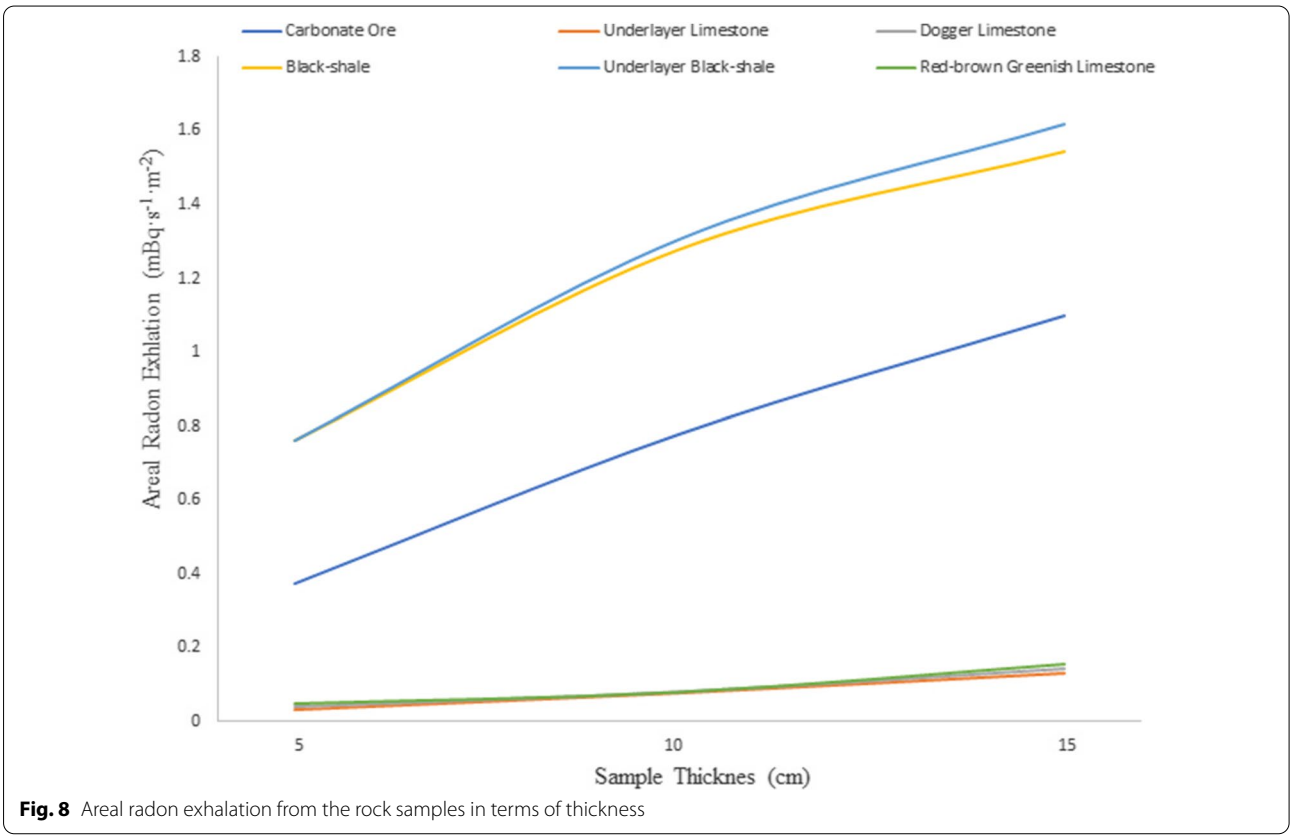

Fig. 8 Areal radon exhalation from the rock samples in terms of thickness

Table 3 Surface radon exhalation from 5 different walls located in the Úrkút mine

Location	Radon exhalation (mBq m^{-2} s^{-1})					
	March	Aug	October	February	Min.–Max	Mean
L-1	1.4 ± 0.2	1.1 ± 0.1	0.9 ± 0.1	1.5 ± 0.2	0.9–1.5	1.2
L-2	1.2 ± 0.2	0.9 ± 0.1	0.8 ± 0.1	1.3 ± 0.1	0.8–1.3	1.0
L-3	1.4 ± 0.2	1 ± 0.1	0.8 ± 0.1	1.4 ± 0.2	0.8–1.4	1.1
L-4	0.9 ± 0.1	0.8 ± 0.1	0.7 ± 0.1	1.1 ± 0.1	0.7–1.1	0.9
L-5	1.1 ± 0.1	1 ± 0.1	0.8 ± 0.1	1.3 ± 0.2	0.8–1.3	1.0

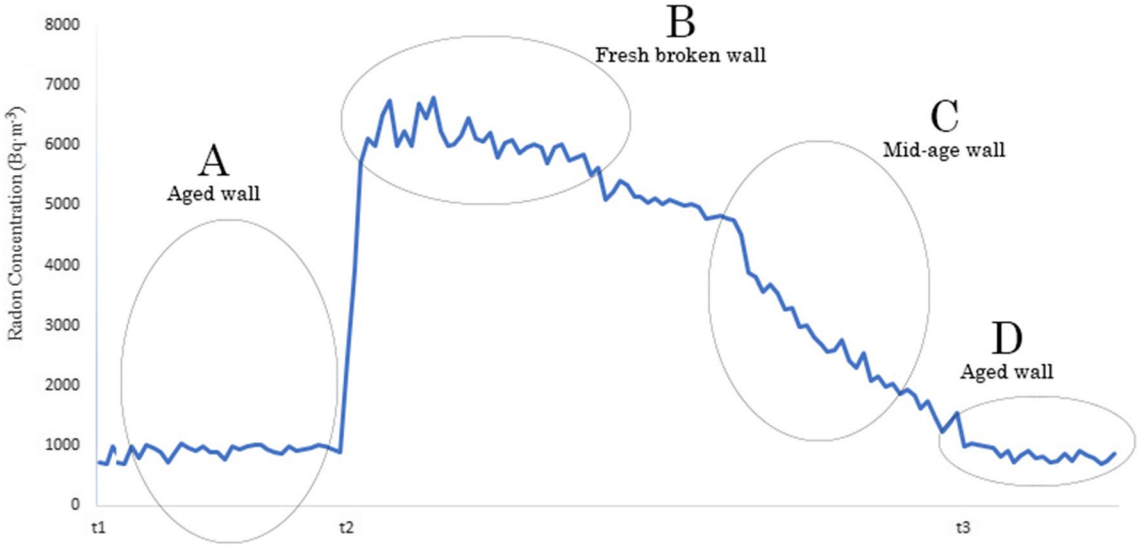

Fig. 9 Released radon as a function of the age of the broken wall

This graph can be used as a mitigation management tool to reduce radon concentration at manganese mines or other underground mines; however, other measurements such as recognizing high potential radon exhalation rocks can be helpful. In the following section, we will address how such an experiment could improve the mitigation system resulting in a successful reduction in the radon concentration.

Performance of optimized mitigation system

Based on the obtained results, to achieve the recommended level of 300 Bq m^{-3} [30], applying the idea of a mobile system to inject fresh air directly to the specific area was considered to mitigate the accumulated radon immediately. Figure 10 shows the performance of the optimized mitigation system in three different locations for 5 days. Plot A shows the radon concentrations with the previously existing mitigation system, and plot B shows the radon concentration after using the mobile mitigation system.

Using the mobile mitigation system dramatically reduced the radon concentration by injecting fresh air directly to the high potential radon route source (new broken rocks). With the regular mitigation system, the average radon concentrations during working hours ranged between 400 ± 55 Bq m^{-3} and 650 ± 81 Bq m^{-3}.

During working hours, the mobile mitigation system was used during mining activities such as exploring or digging. During closing time, the regular ventilator was blowing fresh air to the mine galleries with low velocity. Using the optimized mitigation system successfully reduced the radon concentration on that specific area below 300 Bq m^{-3} with an average of 250 ± 41 Bq m^{-3}.

Using the optimized mitigation system, radon concentration could be reduced by injecting fresh air directly when mining activity was undertaken. The measured radon concentration during working hours when the mobile system was conducted is shown in Table 4. The geometric mean of the three locations was in the range of 150 ± 40 Bq·m^{-3} to 216 ± 53 Bq m^{-3} with an average of 205 ± 49 Bq m^{-3}.

Conclusion

In this study, a radioecology survey was conducted in an underground mine (Úrkút manganese mine) in Hungary to identify the potential routes of radon exhalation and its measurement to control the radiation levels safe limits and protect miners from radiation hazards. 36 samples from the six most abundant different rocks were examined for gamma spectrometry and ex situ radon exhalation to determine the contribution of the mullock (the geological structure of the mine walls) and ore rocks in radon exhalation. It was found that the mullock rocks contained a small amount of Ra-226 (underlayer limestone: 4 Bq kg^{-1}, Dogger limestone: 2 Bq kg^{-1}, Puce greenish marl: 4 Bq kg^{-1}); however, black shale, underlayer black shale and carbonate ore, extracted as the manganese ores, showed the highest concentration of Ra-226 (12, 16 and 16 Bq kg^{-1}, respectively) and the highest areal radon exhalation (the average areal exhalation at 15 cm thickness sample: 1.5, 1.6 and 1.2 mBq·s^{-1}·m^{-2}, respectively). The surface radon exhalation from the wall in the

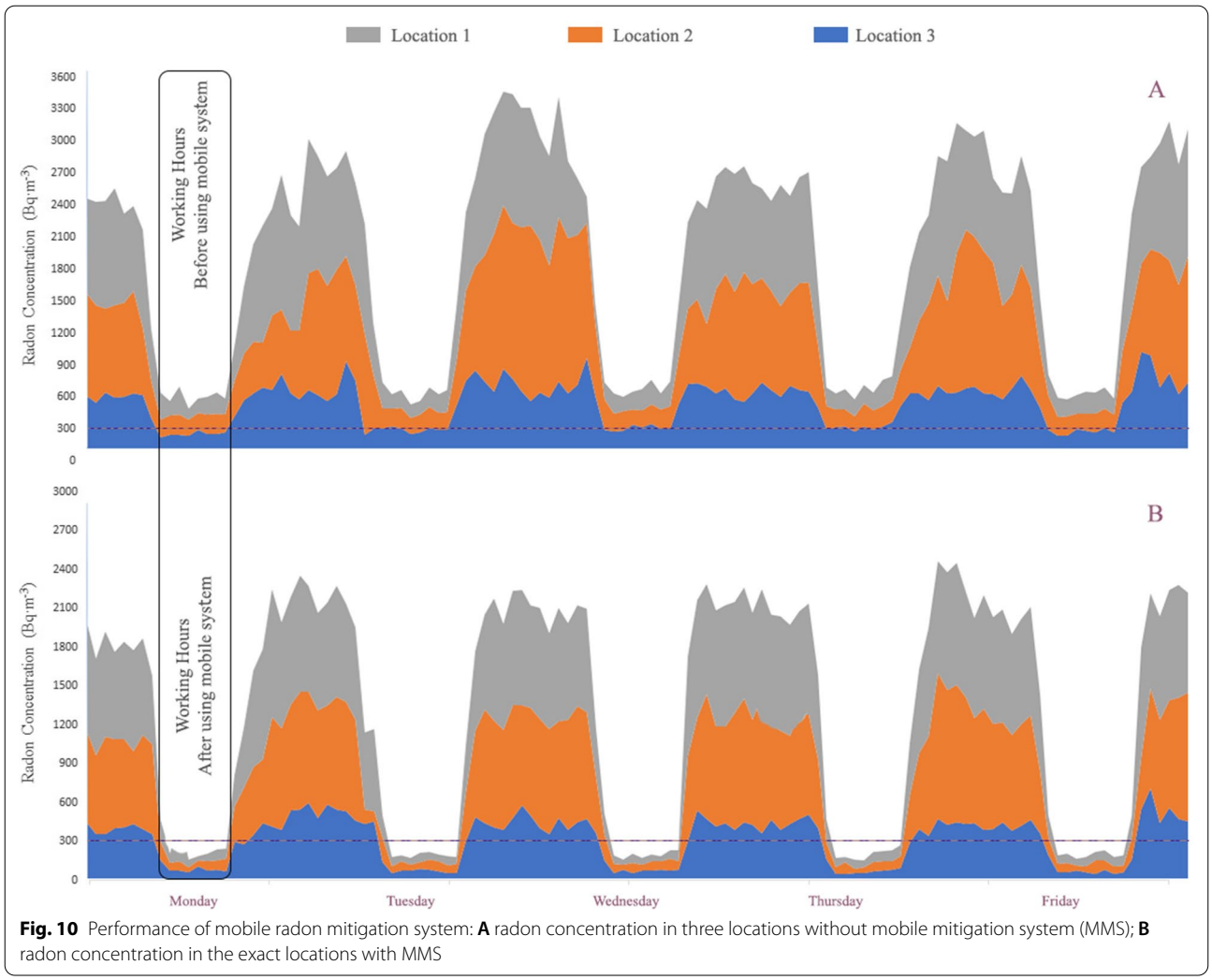

Fig. 10 Performance of mobile radon mitigation system: **A** radon concentration in three locations without mobile mitigation system (MMS); **B** radon concentration in the exact locations with MMS

Table 4 Radon concentration after using optimized mitigation system (Bq m^{-3})

	M 1 Min.–Max. (mean)	M 2 Min.–Max. (mean)	M 3 Min.–Max. (mean)	Three locations (Ave.)
Monday	79 ± 34–415 ± 54 (166 ± 44)	91 ± 48–334 ± 77 (166 ± 43)	170 ± 44–389 ± 95 (216 ± 53)	196 ± 53
Tuesday	103 ± 32–405 ± 89 (161 ± 44)	113 ± 30–463 ± 101 (173 ± 44)	148 ± 41–350 ± 82 (199 ± 49)	191 ± 54
Wednesday	91 ± 32–391 ± 88 (150 ± 40)	91 ± 30–473 ± 103 (176 ± 48)	145 ± 38–383 ± 84 (201 ± 53)	159 ± 44
Thursday	90 ± 30–415 ± 97 (174 ± 47)	91 ± 35–313 ± 77 (160 ± 43)	129 ± 37–402 ± 93 (180 ± 49)	185 ± 49
Friday	126 ± 32–405 ± 92 (182 ± 49)	90 ± 35–331 ± 81 (166 ± 43)	130 ± 35–472 ± 97 (186 ± 50)	192 ± 53
Average	166 ± 45	209 ± 44	196 ± 51	
∑ Average	205 ± 49			

five most active mining areas was measured in the range of 0.7 ± 0.1 and 1.5 ± 0.2 mBq s^{-1} m^{-2}. It was found that the ore, fragmented during mining operations, provided a source of higher radon exhalation due to the increased exposed surface area. Exactly after mining activity was undertaken, the released radon from the freshly broken wall significantly increased with an average of about 5900 Bq m^{-3}. Therefore, by identifying the main route of radon into the mine's air, a mobile mitigation system was introduced using a mobile tube connected to the

enforced ventilation to adjust the mitigation as close as possible to the wall of new galleries. The optimized mitigation system could successfully reduce the radon concentration to below 300 Bq m^{-3}.

Acknowledgements
Not applicable.

Authors' contributions
AS and TK planned and designed the research. AS performed experiments, conducted fieldwork, collected and analyzed data. AS and TK wrote the manuscript. TK contributed reagents, materials, analysis tools. All authors read and approved the final manuscript.

Funding
Not applicable.

Availability of data and materials
They are presented in the paper.

Declarations

Competing interests
Not applicable.

Consent for publication
Not applicable.

Ethics approval and consent to participate
Not applicable.

Received: 19 January 2021 Accepted: 20 May 2021
Published online: 29 May 2021

References

1. Lubin JH, Boice JD Jr, Edling C, Hornung RW, Howe GR, Kunz E, Kusiak RA, Morrison HI, Radford EP, Samet JM, Tirmarche M (1995) Lung cancer in radon-exposed miners and estimation of risk from indoor exposure. J Natl Cancer Inst. 87:817–827
2. Darby S, Whitely E, Howe G, Hutchings S, Kusiak R, Lubin J, Morrison H, Tirmarche M, Tomasek L, Radford E et al (1995) Radon and cancers other than lung cancer in underground miners: a collaborative analysis of 11 studies. J Natl Cancer Inst 87:378–384
3. Tirmarche M, Harrison J, Laurier D, Blanchardon E, Paquet F, Marsh J (2012) Risk of lung cancer from radon exposure: contribution of recently published studies of uranium miners. Ann ICRP 41:368–377
4. Axelsson G, Andersson E, Barregard L (2015) Lung cancer risk from radon exposure in dwellings in Sweden: how many cases can be prevented if radon levels are lowered? Cancer Causes Control 26:541–547
5. Duggan M, HowellSoilleux DP (1968) Concentrations of Radon-222 in coal mines in England and Scotland. Nature 219:1149
6. Hewson GS, Ralph MI (1994) An investigation into radiation exposures in underground non-uranium mines in Western Australia. J Radiol Prot 14:359–370
7. Yener G, Küçüktas E (1998) Concentrations of radon and decay products in various underground mines in western Turkey and total efective dose equivalents. Analyst 123:31–34
8. Qureshi AA, Kakar DM, Akram MA, Khattak NU, Tufail M, Mehmood K, Jamil K, Khan HA (2000) Radon concentrations in coal mines of Baluchistan Pakistan. J Environ Radioact 48:203–209
9. Vishnuprasad Rao K, Linga Reddy B, Yadagiri Reddy P, Ramchander RB, Rama Reddy K (2001) Airborne radon and its progeny levels in the coal mines of Godavarikhani, Andhra Pradesh, India. J Radiol Prot 21:259–268
10. Shahrokhi A, Shokraee F, Reza A, Rahimi H (2015) Health risk assessment of household exposure to indoor radon in association with the dwelling's age. J Radiat Prot Res 40:155–161
11. Shahrokhi A, Nagy E, Csordás A, Somlai J, Kovács T (2016) Distribution of indoor radon concentrations between selected Hungarian thermal baths. Nukleonika 61:333–336
12. Műllerová M, Mazur J, Blahušiak P, Grządziel D, Holý K, Kovács T, Kozak K, Nagy E, Neznal M, Neznal M, Shahrokhi A (2016) Preliminary results of radon survey in thermal spas in V4 countries. Nukleonika 61:303–306
13. Polgári M, Hein JR, Németh T, Pál-Molnár E, Vigh T (2013) Celadonite and smectite formation in the Úrkút Mn-carbonate ore. Sed Geol 294:157–163
14. Kovács T, Shahrokhi A, Sas Z, Vigh T, Somlai J (2017) Radon exhalation study of manganese clay residue and usability in brick production. J Environ Radioact 68:15–20
15. Council of the European Union (2014) Council Directive 2013/59/Euratom of 5 December 2013 laying down basic safety standards for protection against the dangers arising from exposure to ionizing radiation, and repealing Directives 89/618/Euratom, 90/641/Euratom, 96/29/Euratom, 97/43/Euratom. Off J Eur Union 57:1–73
16. Műllerová M, Mazur J, Blahušiak P, Grządziel D, Holý K, Kovács T, Kozak K, Csordás A, Neznal M, Neznal M, Shahrokhi A (2016) Indoor radon activity concentration in thermal spas: the comparison of three types of passive radon detectors. J Radioanal Nucl Chem 310:1077–1084
17. Shahrokhi A, Vigh T, Németh C, Csordás A, Kovács T (2017) Radon measurements and dose estimate of workers in a manganese ore mine. Appl Radiat Isot 124:32–37
18. Adelikhah M, Shahrokhi A, Imani M, Chalupnik S, Kovács T (2021) Radiological assessment of indoor radon and thoron concentrations and indoor radon map of dwellings in Mashhad, Iran. Int J Environ Res Public Health 18:141
19. Shahrokhi A, Adelikhah M, Imani M, Kovács T (2021) A brief radiological survey and associated occupational exposure to radiation in an open pit slate mine in Kashan, Iran. J Radioanal Nucl Chem. https://doi.org/10.1007/s10967-021-07778-w
20. IAEA (2007) Update of X ray and gamma ray decay data standards for detector calibration and other application: data selection, assessment and evaluation procedures. International Atomic Energy Agency, Vienna
21. Adelikhah M, Shahrokhi A, Chalupnik S, Tóth-Bodrogi E, Kovács T (2020) High level of natural ionizing radiation at a thermal bath in Dehloran, Iran. Heliyon 6:e04297
22. Shahrokhi A, Adelikhah M, Chalupnik S, Kocsis E, Toth-Bodrogi E, Kovács T (2020) Radioactivity of building materials in Mahallat Iran – an area exposed to a high level of natural background radiation – attenuation of external radiation doses. Mater Constr 70:e233
23. Shahrokhi A, Adelikhah M, Chalupnik S, Kovács T (2021) Multivariate statistical approach on distribution of natural and anthropogenic radionuclides and associated radiation indices along the north-western coastline of Aegean Sea Greece. Mar Pollut Bull 163:112009
24. Bíró L, Polgári M, Tóth TM, Vigh T, Kávási N, Sahoo SK (2015) Terrestrial radioisotopes as paleoenvironmental proxies in sedimentary formations. J Radioanal Nucl Chem 306:289–293
25. Hosoda M, Shimo M, Sugino M, Furukawa M, Fukushi M (2007) Effect of soil moisture content on radon and thoron exhalation. J Nucl Sci Technol 44:664–672
26. Harb S, Ahmed NK, Elnobi S (2016) Efect of grain size on the radon exhalation rate and emanation coeicient of soil, phosphate and building material samples. J Nucl Part Phys 6:80–87
27. Várhegyi A, Somlai J, Sas Z (2012) Radon migration model for covering U mine and ore processing tailings. Rom J Phys 58:298–310
28. Schumann RR, Gundersen LC (1996) Geologic and climatic controls on the radon emanation coeicient. Environ Int 22:439–446
29. Barton T, Ziemer P (1986) The efects of particle size and moisture content on the emanation of Rn from coal ash. Health Phys 50:581–588
30. ICRP (2017) Occupational intakes of radionuclides: Part 3. ICRP Publication 137. Ann ICRP 46:1–486

Publisher's Note